GEOELECTRICAL AND PETROPHYSICAL STUDIES ON THE OCCURRENCE OF GROUNDWATER IN EL IMAYID AREA, NORTHWESTERN COAST OF EGYPT

Abd Allatief, T.A.; G.H. Galal and A.M.A. Youssef Geophysics Dept., Desert Research Center, El-Matareya, Cairo, Egypt.

> El Imayid area exhibits various activities, such as a touristic ones along the coast and agricultural activity along the frontal plain. The study area depends partially on the fresh water line that passes from Alexandria to Mersa Matruh for domestic uses only. There is a deficiency in water resources for further agricultural and touristic development. Consequently, groundwater potentiality has been studied in El Imavid area. The study for this area is carried out though by two kinds of investigations; one in the field, using the geoelectrical survey through with 15 Vertical Electrical Sounding distributed along three profiles to detect the aquifer depth and extension, and the other in the laboratory using the petrophysical measurements for 14 oolitic limestone samples to clarify the aquifer characteristics. Petrophysical tools are used to study the water collecting characteristics of the oolitic limestone aguifer which is the main aguifer along the coast. Geoelectrical study is used for the subsurface groundwater along the different conditions from north (coast) to south. The geoelectrical results clarify that the two northern ridges are the best places for the drilling of water wells. Water should be discharged carefully from these wells to avoid fresh water depletion or salinization. The petrophysical results clarify that groundwater has easier vertical percolation than horizontal movement. This helps the development of the aguifer and protect it from seepage to the sea with restricted sea water intrusion effect.

Keywords: geophysics, geoelectric, petrophysics, groundwater, Egypt.

The area occupies a portion of the Mediterranean littoral region which is characterized by a low relief varying from the sea level up to about 100 m (Fig. 1). Several authors studied this region as Shata (1953, 1955 and 1957).

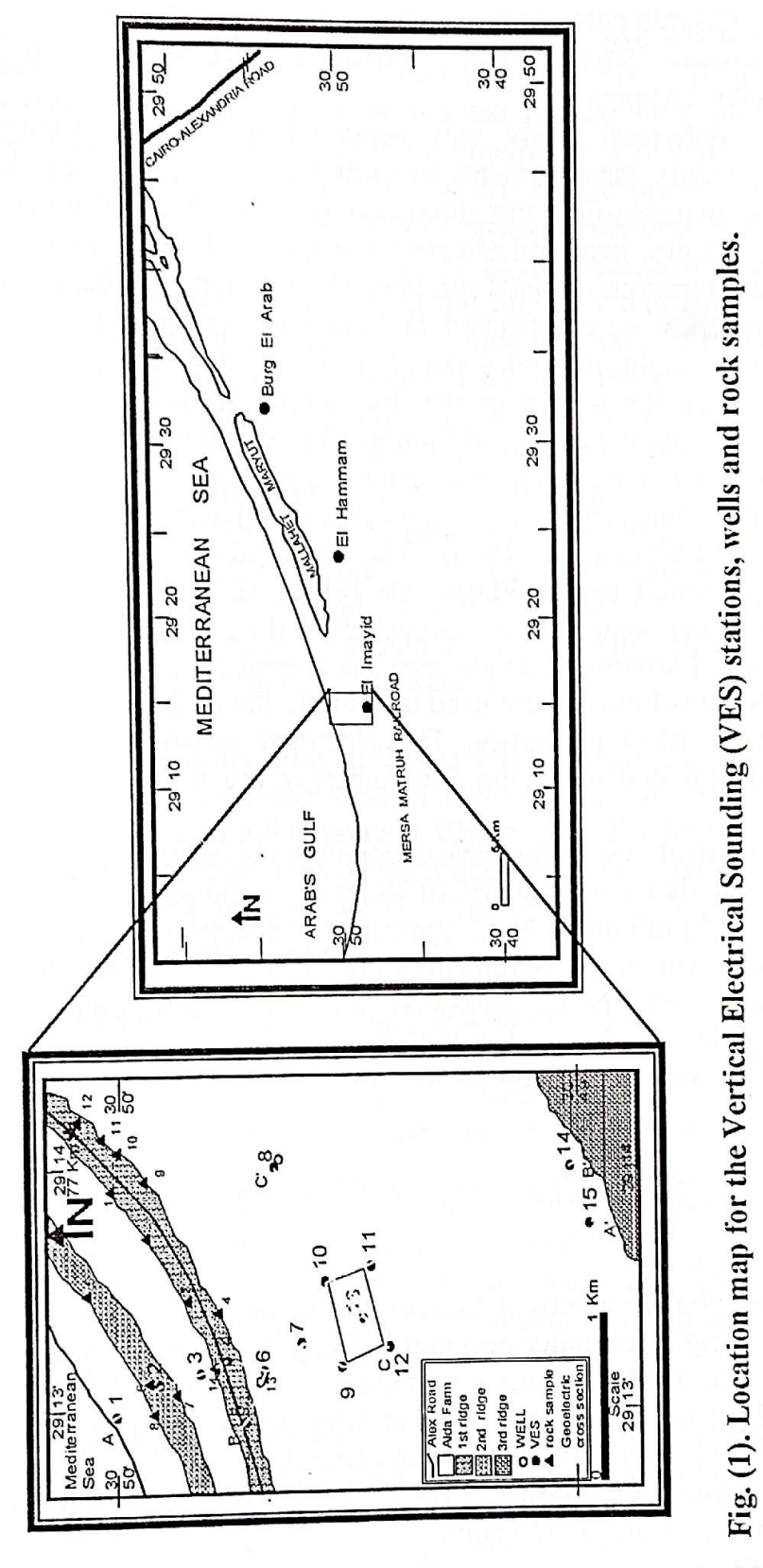
Shukri et al. (1956), Said (1962 and 1990), Hammad (1966), Haraga (1967), Sayed (1967), Bayoumi and Sayed (1971 and 1972), Talaat (1973) and Galal (1995). The main physiographic units characterizing the area from north to south are: the coastal plain, the frontal plain and the table land.

- 1- The coastal plain comprises three ridges and two depressions in between. The three elongate limestone ridges run parallel to the present shore and are composed of white onlitic sand grains that vary from uncemented semifriable to cemented hard ones. The ridges vary in age from Sicilian to Monasterian (Shukri et al., 1956). The first ridge (the near shore ridge) rises 10 20 m above sea level. This height increases in the southern ridges to 35 m (the third ridge). The first depression (the near-shore depression) runs parallel to the present shore line between the first and second ridges. Its surface is almost flat with some slight undulations. Its width is varying from few hundred meters to one kilometer. The second depression occupies the area between the second and the third ridges with a width varying between 2 and 5.
- 2-The frontal plain occupies the area between the third ridge and the table land. This plain is an alluvial plain (Shata 1953, 1955 and 1971).
- 3-The table land represents the plateau to the south of the area which is formed of sandy limestone of Hagif Formation (Pliocene and Pliopleistocene), (Shata, 1957 and El Ghazawi, 1982).

MATERIALS AND METHODS

This study includes geoelectrical field measurements along the different geomorphological units from north to south through 15 vertical electrical soundings (VES), in addition to petrophysical laboratory measurements on oolitic limestone samples from 14 sites, mainly from the first and second ridges (Fig. 1).

The geoelectrical study was carried out through 15 VES where two stations are conducted nearby the present Sawany (hand dug wells) to obtain parametric measurements. Parametric measurements are considered as a base for the quantitative interpretation of the field curves to verify the results. The Schlumberger 4-electrode configuration was used with current electrodes half separation (AB/2) ranging from 300 m to 1500 m. The direct current resistivity meter (Terrameter SAS 4000) was used for the geoelectrical survey. This instrument measures the apparent resistance with high accuracy. Topographic land survey was carried out in order to determine the accurate locations and the ground elevations of VES stations.



Egyptian J. Desert Res., 52, No. 2 (2002)

Field measurements were plotted as VES curves showing the relationship between the apparent resistivity (pa) in Ohm.m on a

bilogarithmic scale (Appendix).

The petrophysical study was achieved through preparing rock samples for laboratory measurements by cutting into suitable size, cleaning and drying. The petrophysical measurements included the determination of bulk and grain density, total and effective porosity and electrical resistivity at three salt concentrations of NaCl solution. The relationships between these different parameters were constructed. Bulk density can be obtained by the ratio between the weight of the dry sample to its volume. The grain density is the ratio between the weight of the dry sample grains to their volume which is obtained from the displaced fluid by the sample grains. Calculating the total porosity (Φt) was done by using the coating technique and the imerssion method while effective porosity (Φ e) was determined by using the saturation method (Amyx et al., 1960). The electrical resistivity of the rock samples was measured using Wheatstone bridge (EKM Type: YTWK-1 apparatus). Six water samples were collected by the authors from different water points in and around the study area for chemical considerations. The equivalent of NaCl solutions were used to saturate the rock samples through measuring the electrical properties. The electrical resistivity of that salt solution was determined using the Schlumberger log interpretation charts (1984).

The electrical resistivity measurements were carried out for three salt solutions, namely a maximum of 10.38 gm/l, a minimum of 0.427 gm/l and a mean of 5.44 gm/l of the NaCl equivalent concentrations. The studied samples were oriented, so measurements were carried out in three directions (north-south direction "N-S", east-west direction "E-W" and vertical direction "V"). These electrical resistivity measurements were used to calculate the formation resistivity factor, the effective directional porosity and tortuosity.

RESULTS AND DISCUSSION

Geoelectrical Study

The quantitative interpretation of the measured field curves was carried out by using a computer program RESIST (Vander Velpen, B.P.A., 1988) for non automatic iteration method in which the field data are compared with data calculated from an assumed layer model. In the construction of such model, the information from the hand dug wells nearby the farm and the available information about the regional and local geologic setting of the area were taken into consideration.

Geoelectrical Results

The quantitative interpretation of the field curves revealed that the

geoelectrical succession is formed of a number of layers which are grouped into 4 main zones. The upper zones (zone "A" and zone "B") are dry. Zone "A" consists of few thin layers which are formed from alluvial deposits (calcareous sand, clay and marl) and in some places affected by evaporites to form sabkha (saline soil). Zone "B" is dry oolitic limestone forming the ridges. Zones "C and D" are the water bearing-formations in the study area. Zone "C" represents the upper part of the aquifer which mostly ranges from fresh to brackish water depending on the lithology and depth. represents the lower part of the aquifer which is formed of brackish to saline groundwater depending on its depth and location from the sea. In general, groundwater salinity increases with depth and also towards the sea. geoelectrical cross sections were constructed illustrating the different conditions along the different geomorphologic units in the study area. The geoelectrical cross sections AA' and BB' (Figs. 2 and 3) cross the area in N-S direction. On the other hand, the geoelectrical cross section C-C' (Fig. 4) crosses the south plain of the study area in E-W direction. Along these cross sections the whole detected succession in the area is presented. The detected 4 zones are described from top downwards as follows:

Zone (A)

It consists of dry alluvial deposits in the depressions. This zone has its maximum resistivity value of 8290 Ohm.m at VES No. 6 and its minimum value of 3.8 Ohm.m at VES No. 9. The low resistivity value reflects the effect of sabkha. The thickness of this zone varies from 3m at VES No. 12 to 2 m at VES No. 7. The thickness of this zone represents the depth to aquifer in the depressions.

Zone (B)

It consists of dry oolitic limestone in the front two ridges. This zone has its maximum resistivity value of 95 Ohm.m at VES No. 5 and its minimum value of 1.1 Ohm.m at VES No. 2. This wide range of resistivity values reflects the effect of the chemical composition of the cement between the oolites. The thickness of this zone varies from 7.5 m at VES No. 1 to 18 m at VES No. 4. The thickness of this zone represents the depth to water at the two front ridges. The extremely low resistivity of this dry rock is either due water capillary (especially in depressions) or a residual water content from percolation during rainfall season at winter (as in ridges).

Zone (C)

It represents the upper water-bearing zone under the ridge. Its water quality ranges from 890 ppm to 2000 ppm (wells of Sheikh Fadl and Khamis Ragab respectively) which depends on the rate and depth of discharge. This fresh water takes the topography shape with roots under the ridges which disappears in the depressions. The resistivity of this zone is 104 Ohm.m at VES No.10 to 0.7 Ohm.m at VES No.8 and has a thickness ranging from 6

m at VES No. 12 to 44 m at VES No. 15. **Zone (D)**

It represents the lower water bearing zone. Its water quality ranges from 4000 ppm to 10000 ppm (wells of Bonsha and Ragab Masood respectively). It is affected not only by the rate and depth of discharge but also by the presence of sabkha that lead to the increase of salinity. The thickness of this zone is not detected. It has resistivity less than 6.7 Ohm.m.

From the studied geoelectric cross sections, it is clear that for the drilling of water wells the sites of the maximum thickness of the water bearing layers are selected as the best sites. These are achieved at VES stations 15, 4 and 2 (cross section A-A') and 11 and 10 (cross sections B-B' and C-C'; Figs. 3 and 4) respectively. It should be noticed that the careful use of the water of these wells will keep the groundwater from depletion or salinisation.

Petrophysical study

This study includes the storage capacity properties and the electrical properties. Storage capacity properties include direct parameters as total and effective porosity and indirect parameters as grain and bulk density. Electrical properties of rocks are basically dependent upon the compositional as well as the collecting properties of rocks.

Density

Grain density reflects the mineralogical composition i.e. the skeleton of the aquifer. On the other hand, the bulk density reflects the void space inside the aquifer skeleton. The laboratory measurements for both parameters reveal that the bulk density ranges from 1.1 gm/cm³ to 2.35 gm/cm³ while the grain density ranges from 1.44 gm/cm³ to 2.56 gm/cm³ (Table 1).

TABLE (1). The statistical results of the studied bulk and grain densities.

Density type	Max.	Min.	Mean	Standard deviation
Bulk Density (gm/l)	2.35	1.10	2.778	0.3157
Grain Density (gm/l)	2.56	1.44	2.675	0.2952

The low values of grain density may be explained as oolites cover microporosity of the oolitic structure. Oolitic limestone has a wide range of grain density and consequently bulk density. This wide range of density values means heterogeneity of the oolits' structure and rock texture. Areal distribution contour maps for grain and bulk densities have similar distribution where their values decrease to the northwest and west direction (Fig. 5).

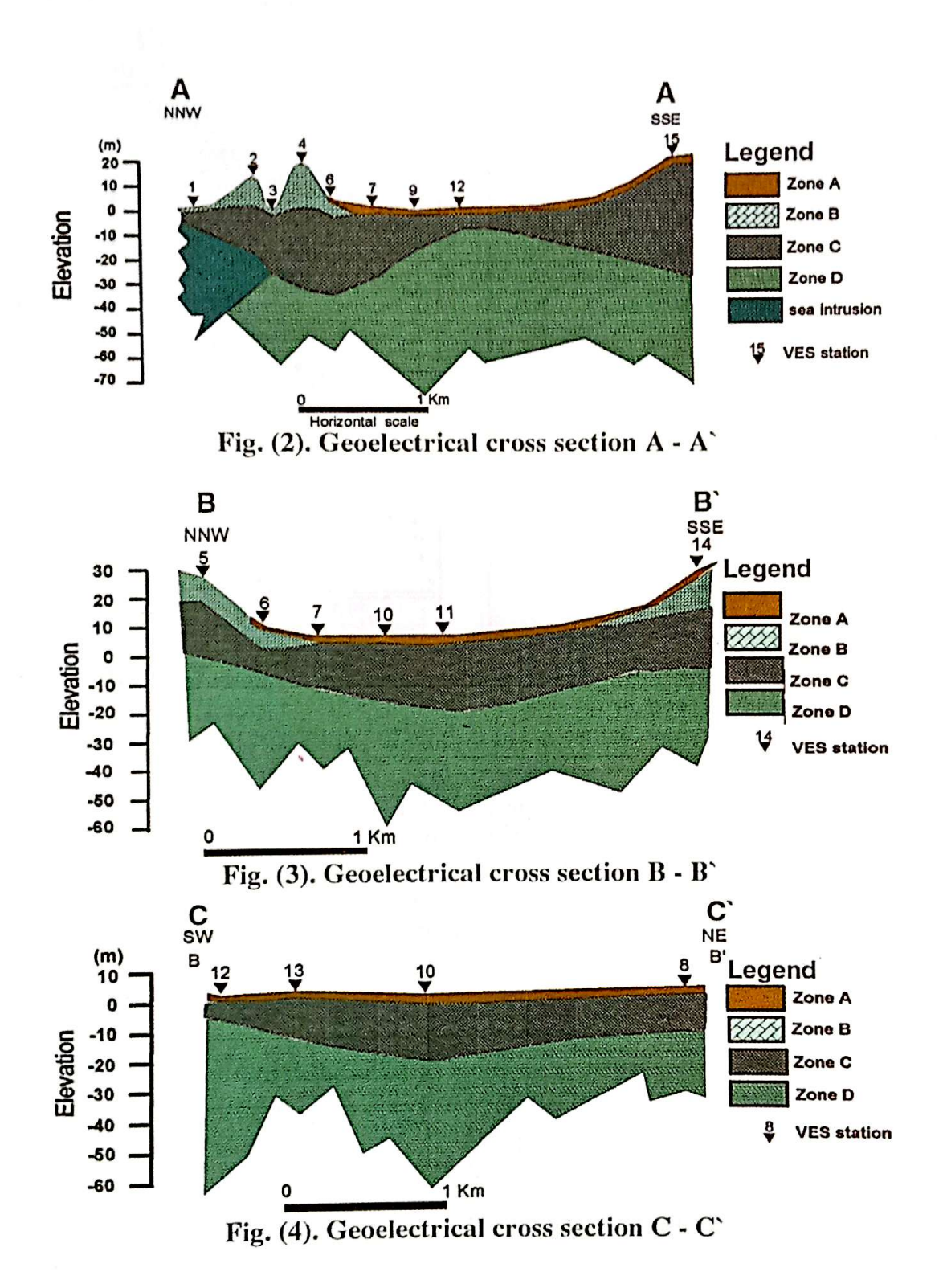


Fig. (4). Geoelectrical cross section C-C

Egyptian J. Desert Res., **52**, No.2 (2002)

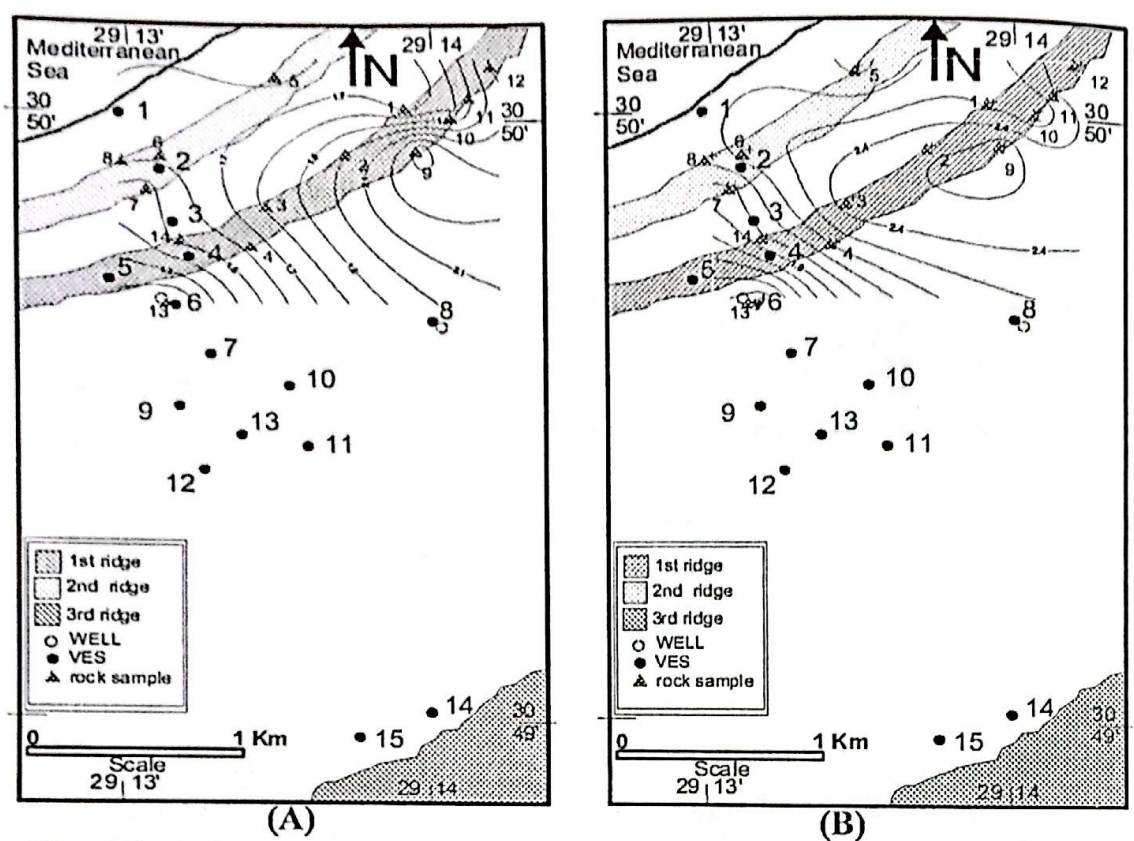


Fig. (5). Iso-contour map of the bulk density (A) and grain density (B).

Porosity

Total porosity reflects the available space for storing water in the aquifer. On the other hand, the effective porosity reflects the available space to extract groundwater from the aquifer.

Total porosity (Φ t) ranges from 10.05 % to 35.33 % and its effective porosity ranges from 8.16 % to 29.10 % (Table 2).

TABLE (2). The statistical results of the total and effective porosities.

Porosity types	Max.	Min.	mean	Standard deviation
Total Porosity	35.33	10.05	20.91	0.06656
Effective Porosity	29.10	8.16	22.37	0.05899

The wide range of total and effective porosity values reflect the effect of cement between oolites. On the other hand, the varying difference between total and effective porosity reflects the heterogeneous effect of cement on the distribution of pores inside the oolitic rocks and sediments of the studied samples. Areal distribution contour maps of the total and

effective porosities have the same behaviour where the values increase toward the northwest direction. This distribution means that the aquifer storage capacity increases in the same direction to the northwest (Fig. 6).

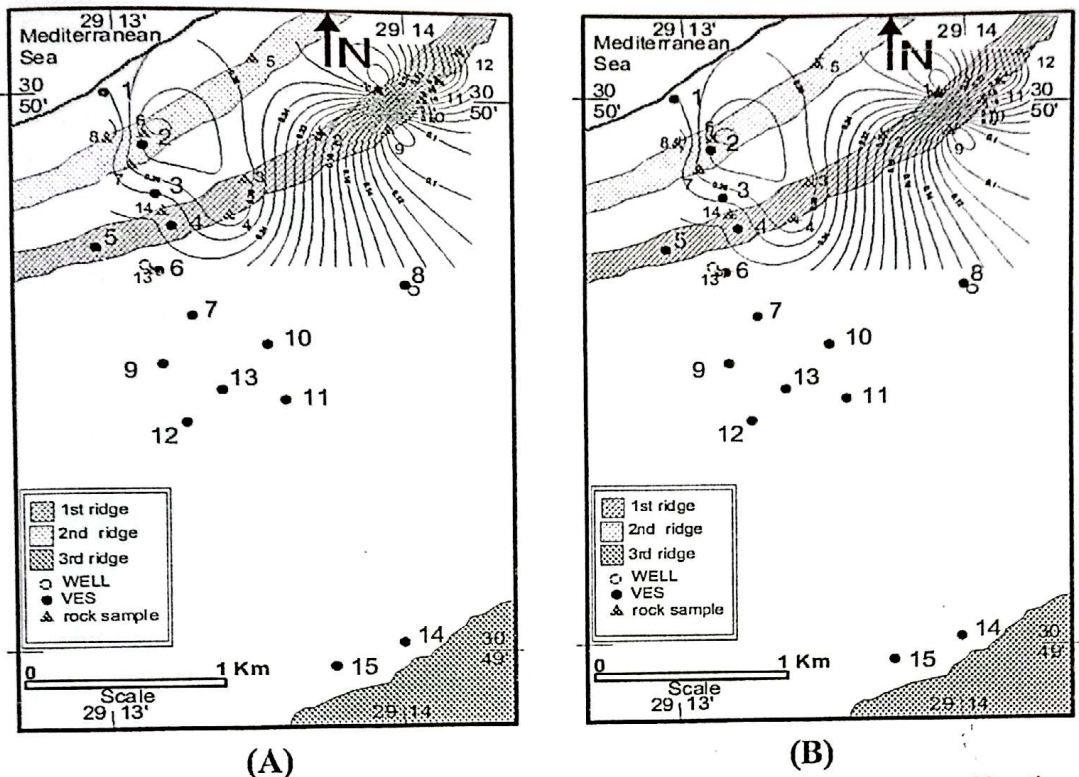


Fig. (6). Iso-contour map of the total porosity (A) and effective porosity (B).

Relation Between Total Porosity and Bulk Density

The relation between the bulk density ρ_b and total porosity Φ_t is a reversible relation (Fig.7) where the total porosity increases by the decrease of bulk density and the regression line equation has been calculated for each rock type as follows $\rho_b = 2.63594 - 4.04382 \Phi_t$ r = -0.570991

This relation has low correlation coefficient (r) as a result of heterogeneity of the studied samples. This is due to the internal stucture, texture and the effect of the cement chemical composition which differs from the rock skeleton.

Electrical Properties

The resistivity of a rock (ρ) is defined by the following equation:

 $\rho = R.(A/L)$

where: ρ = resistivity in Ohm.m.; R = resistance in Ohm.; A = cross sectional area of the conductor in m², L = length of the conductor in m.

According to Amyx et al. (1960), the resistivity of the rock sample is usually expressed in Ohm.m, which is used in this study. The electric

resistivity of a rock depends mainly on the mineral composition, texture and structure of the rock grains, the amount and type of saturating fluids, and the temperature and pressure of the prevailing conditions. The electric resistivity has been measured in three salt solutions for three main directions (Table 3).

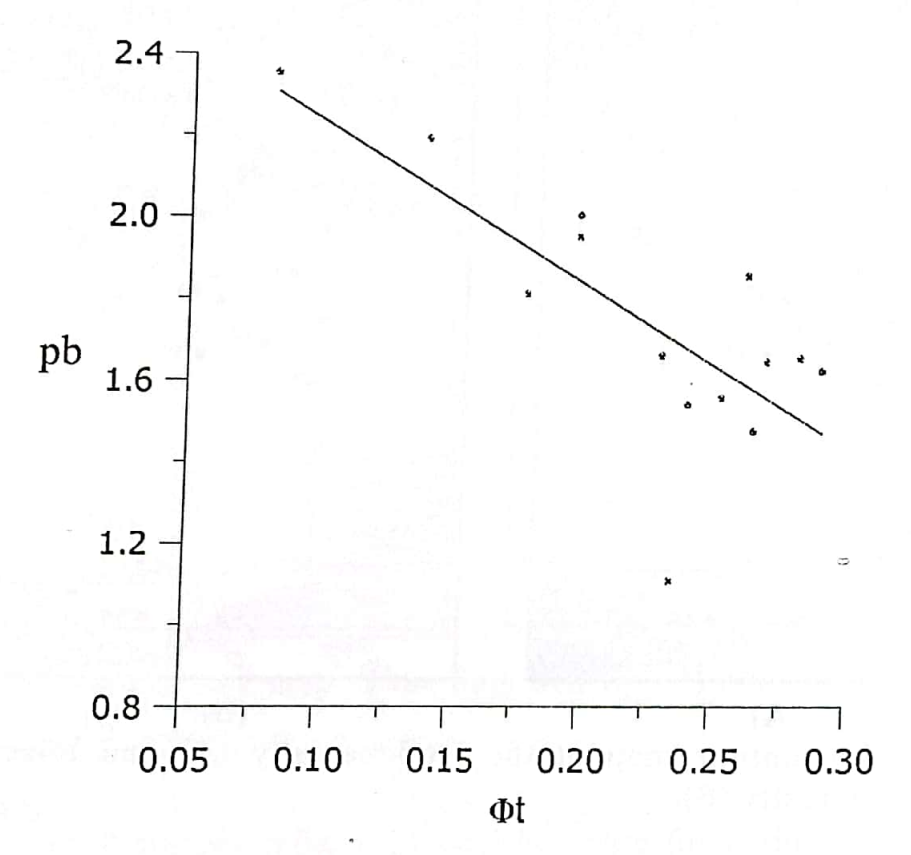


Fig. (7). The relation between total porosity (Φ t) and bulk density (Pb) TABLE (3). The statistical results for the studied electrical resistivity.

Brine conce- ntration (gm/l)	Direction	Max.	Min.	Mean	St. dev.
	N-S	95.9489	21.1899	38.1625	22.5633
0.427	E-W	89.3719	13.7326	33.6013	22,7954
0.427	Vertical	91.2237	14.3328	29.3704	19.5033
5.44	N-S	19.7979	9.4328	15.6091	2.7958
	E-W	19.8781	8.4045	14.1452	2.7320
	Vertical	17.7867	8.0493	12.6585	3.2064
10.38	N-S	15.0502	2.4860	9.6932	4.5026
	E-W	12.9187	2.1925	8.4538	3.7812
	Vertical	14.7895	1.7248	7.7473	4.1994

Egyptian J. Desert Res., 52, No.2 (2002)

The measured mean electrical resistivity in all the saturating salt solutions indicate that the horizontal directions (NS and EW) have higher values than the vertical direction. This means that sea water intrusion effect on the aquifer is limited.

Formation Resistivity Factor (F)

Formation resistivity factor is a function of the effective path length of the electric current flow and the effective cross-sectional area available for electric conduction (Pantode and Wyllie, 1950).

The formation resistivity factor (F) is defined as the ratio between the electric resistivity of a rock sample saturated with a conducting salt solution (ρ_o) and the resistivity of the salt solution (ρ_w) saturating such rock samples . It can be computed from the equation of Archie (1942) as:

$$F = \rho_o / \rho_w$$

The formation resistivity factor is measured for each salt solution at the three directions (Table 4).

Table (4). The statistical re	esults for the	formation resistivity	factor.
-------------------------------	----------------	-----------------------	---------

Brine concentration (gm/l)	Direction	Max.	Min.	mean	St. dev.
18	N-S	7.3807	1.6299	2.9356	1.7356
_	E-W	6.8748	1.0564	2.5847	1.7535
0.427	Vertical	7.0172	1.1025	2.2593	1.5003
	N-S	19.7979	9.4328	15.6091	2.7958
	E-W	19.9791	8.4045	14.1099	2.8503
5.44	Vertical	17.7868	8.0493	12.6585	3.2064
	N-S	32.0218	5.2893	20,6239	9.5802
	E-W	27.4865	4,6649	17.9868	8.0451
10.38	Vertical	31.4671	3.6699	16.4836	8.9348

The values of formation resistivity factor increase by increasing salinity of the saturating salt solution where they are related to the decrease of ρ_w . Formation resistivity factor records the lowest value in vertical direction and the highest one in the north-south direction.

Relation Between the Formation Resistivity Factor (F) and Porosity (Φ) Archie (1942) studied the relation between the formation resistivity factor and the porosity of rocks and proposed the following equation:

$$F = a \Phi^{-m}$$

Where : F = Formation resistivity factor, $\Phi = effective$ rock porosity, m = cementation exponent, a = a function of tortuosity.

This relation is studied to delineate the changes in the cementation exponent (m), tortuosity function (a) and the correlation coefficient (r)

through the different directions and saturating salt solutions where arenite and limestone represent significant relations but calcareous sandstone is insignificant (Table 5 and Fig. 8).

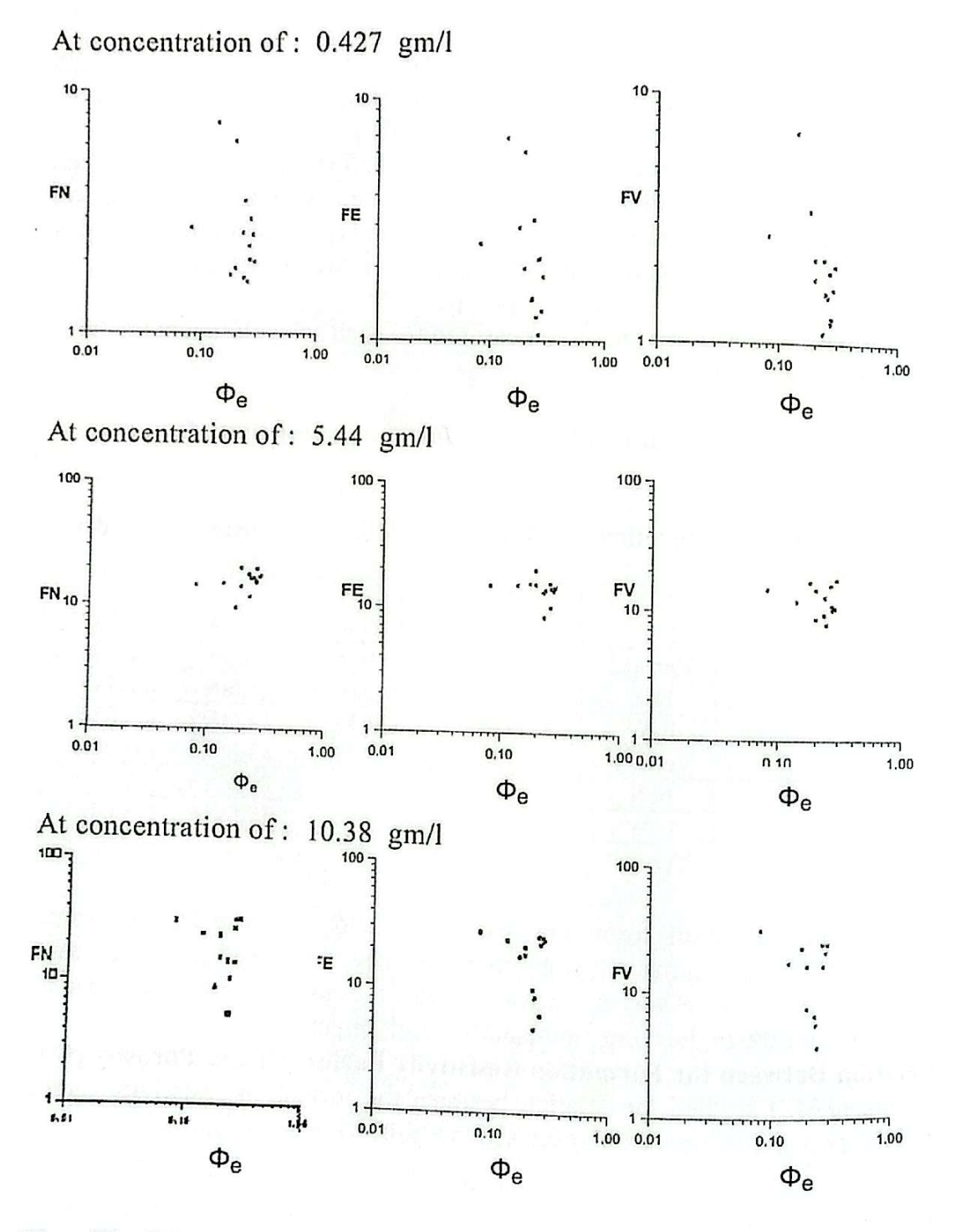


Fig. (8). The relation between effective porosity Φ e and formation resistivity factor (F) at the three salt solutions for the three main directions.

TABLE (5). The equations of the studied formation resistivity factor in relation to porosity.

Concentration (gm/l)	Direction N – S	Direction E - W	Direction Vertical
0.427	$F = 1.6165 \Phi^{-0.3569}$ $r = 0.0422$	$F = 0.7577 \Phi^{-0.7196}$ $r = 0.2229$	$F = 1.2382 \Phi - 0.4417$ r = 0.0472
5.44	$F = 17.7187 \Phi^{-0.1157}$ $r = 0.0305$	$F = 11.2517 \Phi^{-0.1399}$ r = 0.0615	$F = 10.6831 \Phi - 0.1014$ r = 0.0191
10.38	$F = 10.9819 \Phi^{-0.2785}$ $r = 0.02282$	$F = 5.8171 \Phi^{-2.80657}$ $r = 0.0932$	$F = 0.992901 \Phi - 2.52304$ r = 0.1035

The values record high cementation factor (m) and low multiplier factor (a) at the salt solution of 10.38 gm/L and the reverse is recorded at 5.44 gm/L. The correlation coefficient (r) records the highest values at E-W direction which can be declared by the genesis of solitic limestone. Its formation is by agitating current of the sea. The agitating current of the sea is - in this case - along the north-south direction i.e. the line of change in the sedimentation condition changes in north-south direction whereas the line of homogeneity is perpendicular to the sea current direction in east-west direction.

Effective directional porosity (Φ ed)

Klinkenberg (1951) gave the term "effective directional porosity" to the ratio A'L/AL', where A and L are the cross-sectional area and the length of the sample but A' and L' represent the same parameters for void path. The effective directional porosity is the reciprocal of the formation resistivity factor (F) as stated by Winsauer et al. (1953).

The effective directional porosity values are calculated from formation factor determined at highest concentration (10.38 gm/1) of the saturating salt solution to avoid the shaliness effect (Table 6).

TABLE (6). The statistical results of the effective directional norosity.

Direction	Max.	Min.	Mean	Standard deviation
N-S	9.3173	1.2444	4.5946	2.8424
E-W	7.0930	1.0975	3.8677	2.1406
Vertical	7.1250	0.8840	3.4579	2.1459

Effective direction porosity is slightly higher in the horizontal directions (N-S and E-W) than in the vertical direction but their mean values for the studied aquifer have small variation that is clear from the standard deviation values (Table 6). The areal distribution contour maps

for the effective directional porosity (Fig. 9) have similar changes where their values increase due north west direction.

Tortuosity (t)

Tortuosity of the pores within a rock is defined as the ratio of the statistical mean of tortuous length (L') of the pore channels traversed by an electric current flowing from one to another of two parallel planes with a water-saturating rock to the distance (L) between the planes (Kobranova, 1962).

Numerically, the tortuosity (t) can be related to the formation factor (F) and porosity (Φ) through the expression $\int_{0}^{\infty} t = \int_{0}^{\infty} \Phi$ (Mohamed and Zeidan, 1978).

TABLE (7). The statistical results for the studied tortuosity.

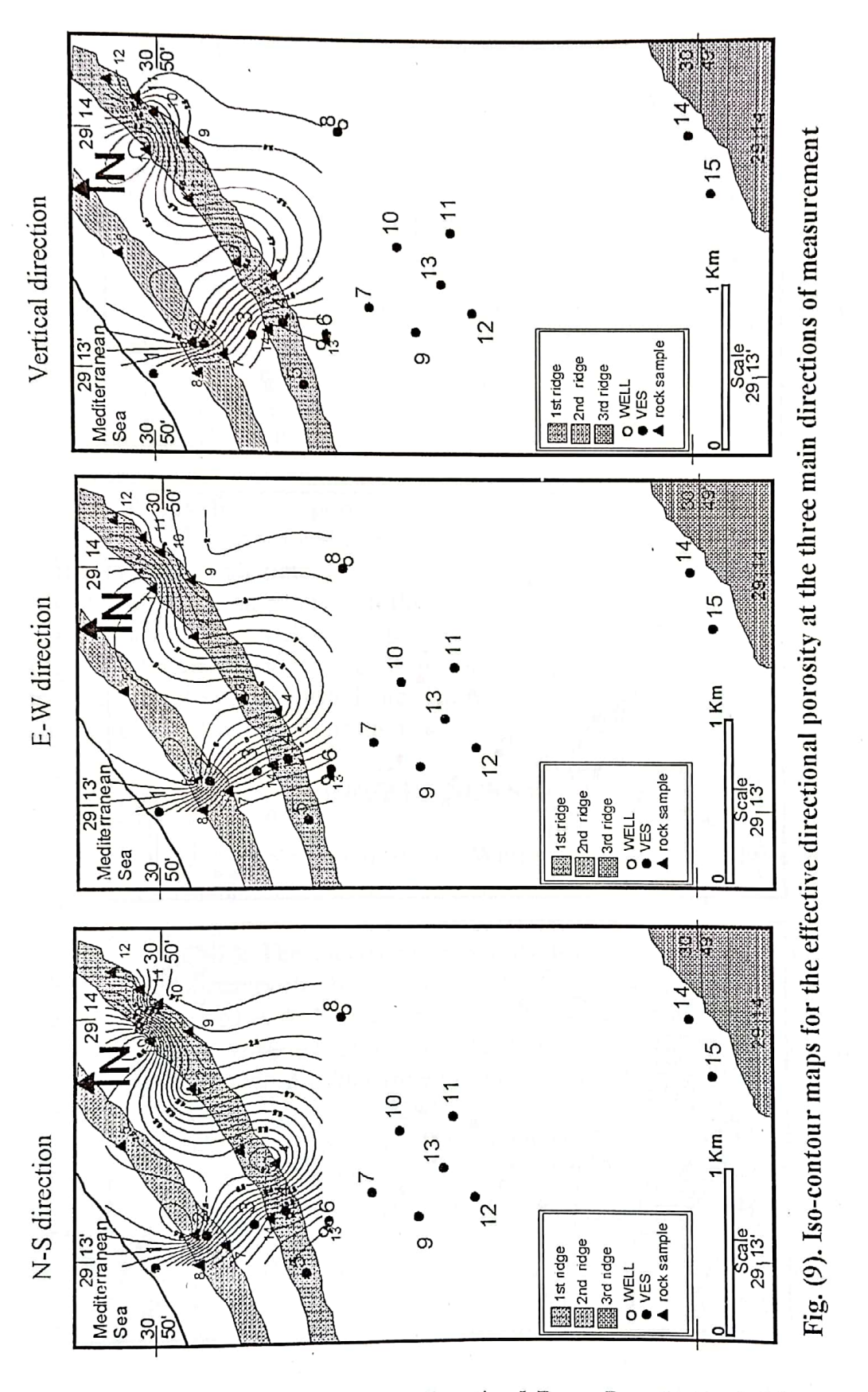
Direction	Max.	Min.	Mean	Standard deviation
N-S	3.0524	1.1155	2.0495	0.6535
E-W	2.6633	1.0476	1.8943	0.5502
Vertical	2.6693	1.9402	1.7732	0.5850

From table (7), it is clear that tortuosity is higher in the N-S direction than along the other directions, which retards groundwater flow toward the sea. In addition to this result of the aquifer is protected from sea water invasion. On the other hand, tortuosity is low in the vertical direction which means easy percolation of surface water to the aquifer. The areal distribution contour maps for tortuosity (Fig. 10) have similar changes where their values increase to northwest direction.

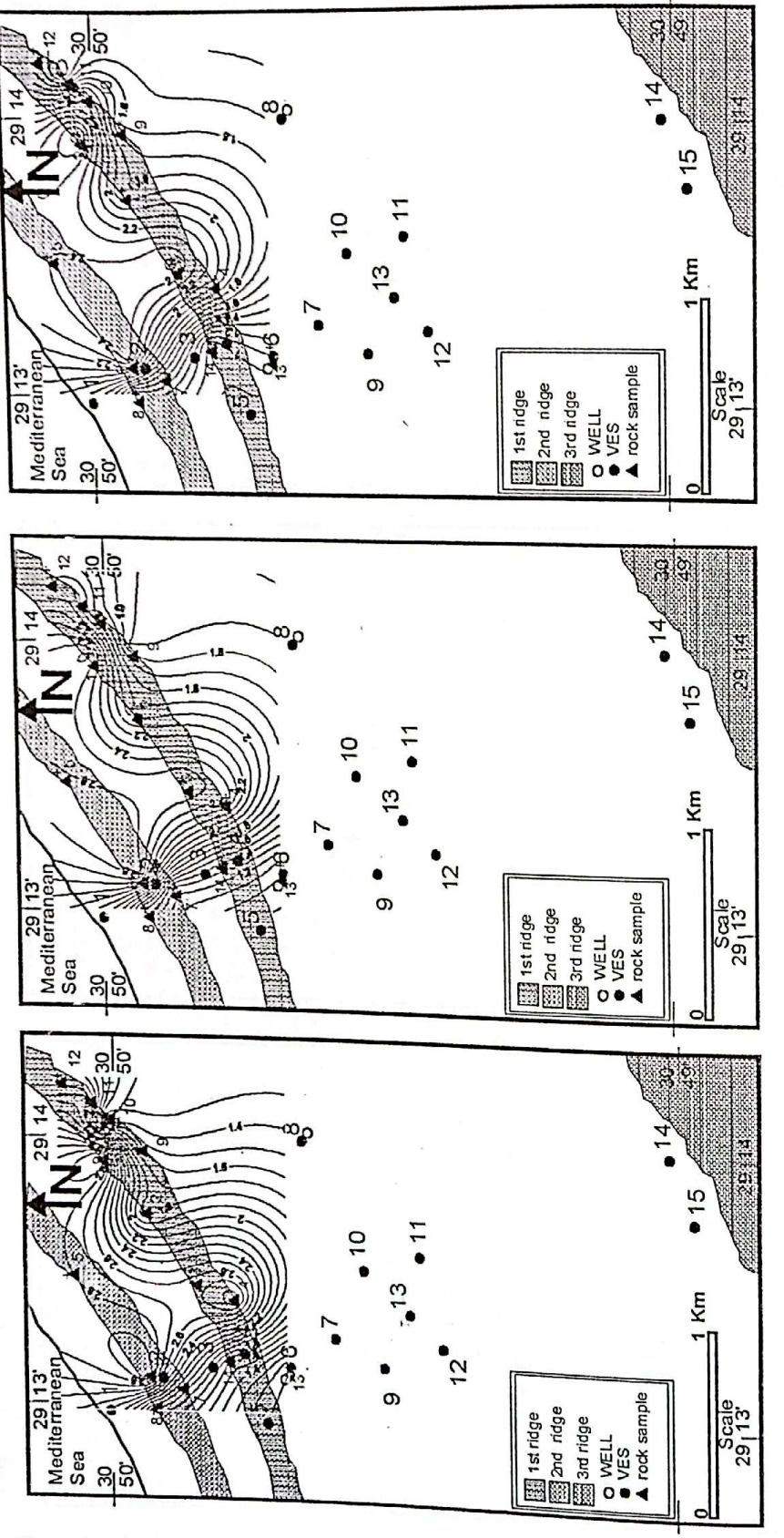
CONCLUSION AND RECOMMENDATIONS

The application of the electrical resistivity sounding method to delineate the groundwater occurrence in the study area revealed the following:

1- The geoelectrical succession consists of four geoelectrical zones. The first two zones (A and B) consist of dry layers. The third zone (C) represents the upper part of the aquifer which consists of fresh water lens in the ridge with a thickness ranging from 44 m to 12 m that follows the topography with roots under the ridges and disappears in the depressions where brackish water with low resistivity exists due to the effect of sabkha. The fourth zone (D) represents the lower part of the aquifer which consists of brackish to saline water-bearing zone reflecting the effect of sea water intrusion.



Egyptian J. Desert Res., 52, No. 2 (2002)



Egyptian J. Desert Res., 52, No. 2 (2002)

Fig. (10). Iso-contour maps for the electrical tortuosity at the three main directions of measurement

- 2- The petrophysical studies indicated high tortuosity and resistivity in the horizontal directions while low values are recorded in the vertical direction. This means that the fluid movement is more difficult in the horizontal direction than in the vertical direction which leads to the following results:
- i- The effect of sea water intrusion on the groundwater is limited.
- ii- Easy vertical percolation of water which facilitates aquifer recharge during the rainfall season.
- iii- Difficult horizontal discharge which help in developing the aquifer and protecting it from seepage to the sea.

The areal distribution contour maps reveal that all the studied petrophysical parameters are related in their change to the direction of sedimentation process that is related to the sea movement from northwest to southeast direction. The studied geoelectric cross sections and the areal distribution maps for the porosity reflect high storage capacity to the northwest. The best sites for the drilling of water wells have been chosen for good quality and high potentiality. These sites are VES stations 4 (cross section A-A') as a first priority, followed by VES station 15 (cross section A-A'; Fig. 2) and 11 and 10 (cross sections B-B' and C-C'; Figs. 3 and 4). It should be noticed that the careful use of groundwater respectively discharged from these suggested sites for the drilled wells will preserve the aquifer from depletion or salinisation.

REFERENCES

- Amyx, J. W.; D. M. Bass and R. L. Whiting (1960). In "Petroleum reservoir engineering". Mc Graw Hill Book Co., Inc., New-York.
- Archie, G. E. (1942). The electrical resistivity log as aid in determining some reservoir characteristics. *Trans. AIME.*, 146: 54-60.
- Bayoumi, A.I. and M.A.A. Sayed (1972). In "A geoephysical study on the groundwater resources of the limestones of Ras El-Hekma area, North Mediteranean coastal zone of Egypt". Geol. Jb., C2, Hannover, p. 261-267.
- Bayoumi, A.I. and M.A.A. Sayed (1971). Geoelectrical characteristics of the water bearing formation, Ras El-Hekma coastal area, Western Desert, Egypt. Bull. Desert Inst., Egypt, 21(2): 313-325.
- Carver, R.E. (1971). In "Procedure in sedimentary petrology", Wiley-interscience, New York, 653pp.
- El Ghazawi, M.M.M. (1982). Geological studies of the Quaternary Neogene aquifers in the area north west Nile Delta. *M.Sc. Thesis*, Fac. Sci., Al Azhar Univ., Cairo, Egypt.

Galal, H. G. H. (1995). "Geophysical studies to delineate the geological and hydrogeological conditions in the area between Ras Alam El Rum-Ras Abu Laho - north western coast - Egypt". Ph.D. Thesis, Fac. Sci., Ain Shams Univ., 165 pp.

Hammad, F.A. (1966). The geology of water supplies in Ras El Hekma area, Western Mediterranean Littoral, Egypt. M.Sc. Thesis,

Fac. Sci., Cairo University, Egypt.

Haraga, A.A. (1967). Morphological and physio-chemical studies of Burge El Arab - El Hammam area. M. Sc. Thesis, Fac. Agric., Ain Shams University, Egypt.

Klinkenberg, L.J. (1951). Analogy between diffusion and electrical conductivity in porous rocks", Bull. Geol. Soc. Amer., vol. 62.

Kobranova, V.N. (1962). In "Physical properties of rocks" (in Russian), Gestoptechizdat, Moscow, 490 pp.

Mohamed, S. S. and S. Zeidan (1978). An experimental investigation on the relation between diffusion-adsorption activity and some other petrophysical parameters in silty sandstone. Faculty of Petroleum and Mining Engineering Journal, Al Fateh University, Tripoli, Libya. FPMEJ., 1(1): 23-32.

Pantode, H.W. and M.R.J. Wyllie (1950). The presence of conductive solids in reservoir rocks as a factor in electric log interpretation. Trans. AIME., 189: 47-52.

Said, R. (1990). In "The geology of Egypt", A.A. Balkema, Rotterdam, Netherlands, 733pp.

Said, R. (1962). In "The geology of Egypt", Elsevier Publishing, Amsterdam, New York, 377pp.

Sayed, M.A.A. (1967). Geophysical studies on the groundwater resources of Ras El-Hekma area, northern Mediteranean coastal zone of Egypt. M.Sc. Thesis, Fac. Sc., Cairo Univ., Egypt, 129 pp.

Schlumberger (1984). In "Log Interpretation Charts". Schlumberger Limited, Paris, France.

Shata, A.A. (1971). The geomorphology, pedology and hydrogeology of the Mediterranean coastal desert of A.R.E. Proceeding Symposium of the geology of Libya.

Shata, A.A. (1957). Remarks on the physiography of El Ameriya-Maryut area, Bull. Sco. Geogr. d'Egypte, T. 30.

Shata, A.A. (1955). An introductory note on the geology of the northern portion of the western desert of Egypt Bull. Inst. Desert,

Shata, A.A. (1953). New light on the structural development of the western desert of Egypt. Bull. Inst. Desert, Egypt, 3 (1):101-

Shukri, N.M.; G. Philip and R. Said (1956). The geology of the Egyptian J. Desert Res., 52, No.2 (2002)

Mediterranean coast between Rosetta and Bardia.ii.Pleistocene sediments, geomorphology and microfacies. *Bull.Inst.Desert Egypte*, 37: 395 - 433.

Talaat A. A. (1973). Geophysical studies on underground water in some localities between Ras El-Daba and Ras El-Hekma North West coastal zone, *Ph.D. Thesis* Geol. Dept., Fac. Sci., Cairo University, Egypt, 186 pp.

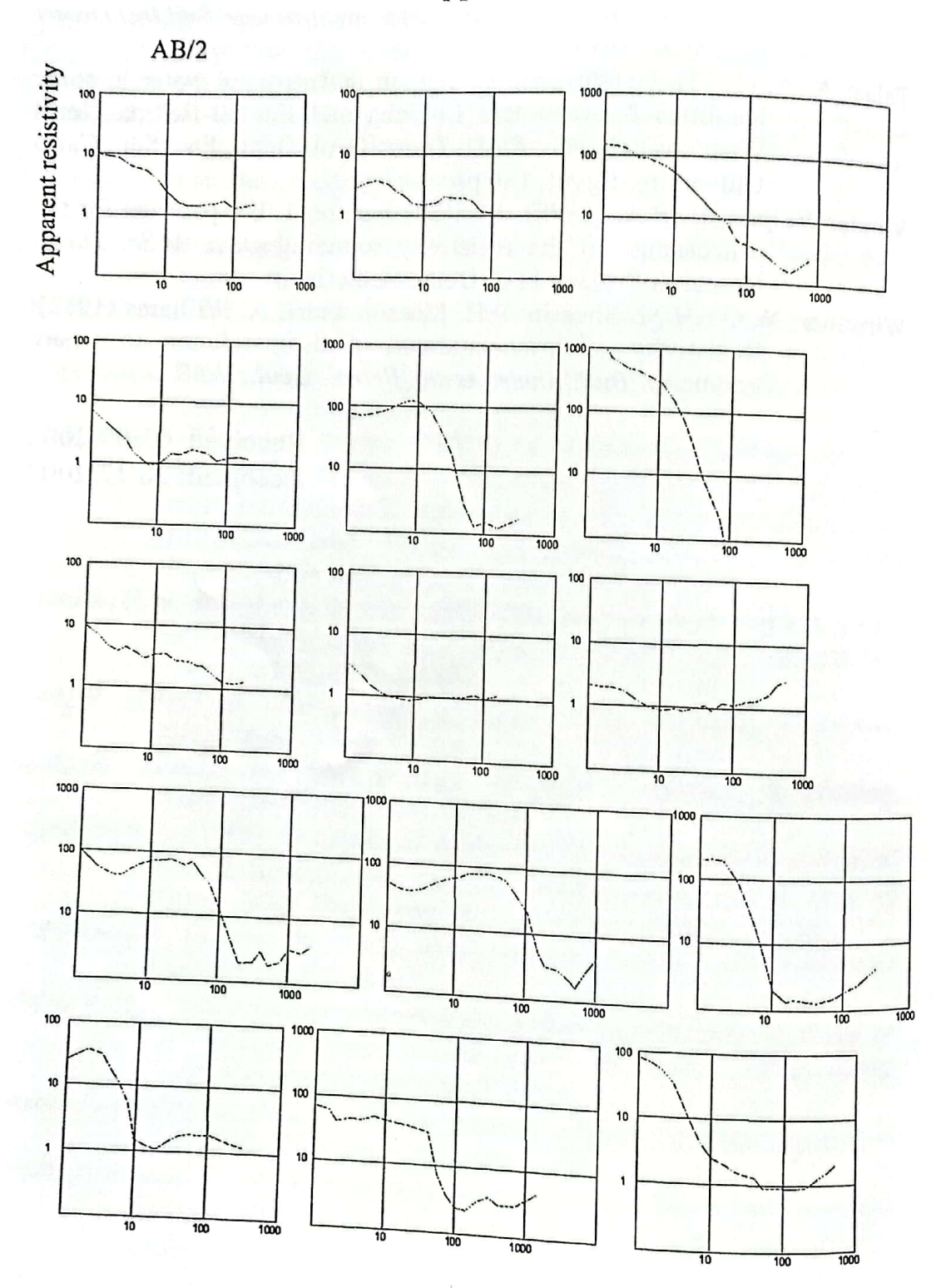
Vander Velpen, B. P.A. (1988). RESIST: version 1.0, a package for the processing of the resistivity sounding Data. M.Sc. Thesis

Research Project, ITC, Delft, Netherland.

Winsauer, W.O.; H.M. Shearin; P.H. Masson and R.A. Williams (1952). Resistivity of brine-saturated sand in relation to pore geometry. *Bull. Amer. Assoc. Petrol. Geol.*, V.40.

Received: 03/09/2002 Accepted: 28/12/2002

Appendix



Egyptian J. Desert Res., 52, No.2 (2002)

دراسات جيوكهربية و بتروفيزيائية على تواجد المياه الجوفية بمنطقة العميد، الساحل الشمالي الغربي لمصر.

طلعت على عبد اللطيف ، جلال حسن جلال ، أحمد يوسف قسم الجيوفيزياء - مركز بحوث الصحراء - المطرية - القاهرة - مصر ·

تقع منطقة الدراسة على الساحل الشمالى الغربى لمصر غرب الحمام بمنطقة العميد عند الكيلو ٧٧ من الاسكندرية حيث تقع منطقة عايدة السياحية و مزرعتها تتميز منطقة الدراسة بخصائص الساحل الشمالى الغربى الجيومورفولوجية من سهل ساحلى منخفض يتكون من شاطئ شمالى يليه للجنوب ثلاثة جروف موازية لساحل البحر مكونه من الحجر الجيرى البطروخي، تفصل بين هذه الجروف منخفضات ضحلة تتأثر أحيانا بالسبخات الجيرى البطروخي، تفصل بين هذه الجروف منخفضات ضحلة تتأثر أحيانا بالسبخات،

لذلك تمت دراسة الظروف الهيدروجيولوجية المختلفة من خلال ١٥ جسة كهربية و من الدراسة الجيوكهربية وجد ان التتابع الجيوكهربي يتكون من اربعة نطاقات نطاقين منهما جافين (1^8 ب) أما النطاقين الثالث و الرابع (1^8 ع) فيحتويان على الماء الخطاق الثالث بسمك يتراوح من 1^8 الى 1^8 الى 1^8 المنخفضات ليصبح ضاربا الى الملوحه بتأثير السبخات أما النطاق الرابع يقع تحت النطاق الثالث بسمك لم يتم تحديده من خلال الجسات، المسبخات ملى ماء يتراوح من ضارب الى الملوحه الى مالح.

كذلك تمت دراسة الجروف الساحلية بتروفيزيائياً من خلال ١٤ موقع لدراسة خزان الحجر الجيرى البطروخي، أوضحت الدراسة البتروفيزيائية أن اتجاه التغير للقيم المختلفة مرتبط باتجاه الترسيب من الشمال الغربي للجنوب الشرقي، هذا بالاضافة الى أن قيم الالتواء و المقاومة الكهربية تزيد في الاتجاه الافقى و تقل في الاتجاه الرأسي، يدل هذا على أن امكانية التخزين من خلال التسرب الرأسي للخزان أسهل من عملية التسرب الأفقى للخزان مما يساعد على تنميته و حفظه من الضياع و حمايته من تأثير مياه البحر،

و من النتائج الجيوكهربيه و خرائط التوزيع لقيم المسامية وجد أن أفضل الاماكن لحفر آبار انتاجيه للمياه الجوفية تكون على الجرفين الساحلي الشمالي حيث افضل جوده للمياه و اعلى امكانية للتخزين بليها الجرف الجنوبي ثم منتصف المنخفض الجنوبي · حيث يراعي السحب المقنن لحماية الخزان من الاستنزاف أو خلطه بالمياه المالحه العميقة أو القادمة من مياه البحر الى الشمال ·